

Magnetism of the $N = 42$ kagomé lattice antiferromagnet

Jürgen Schnack,^{1,*} Jörg Schulenburg,² and Johannes Richter^{3,4,†}

¹*Fakultät für Physik, Universität Bielefeld, Postfach 100131, D-33501 Bielefeld, Germany*

²*Universitätsrechenzentrum, Universität Magdeburg, D-39016 Magdeburg, Germany*

³*Institut für Theoretische Physik, Universität Magdeburg, P.O. Box 4120, D-39016 Magdeburg, Germany*

⁴*Max-Planck-Institut für Physik Komplexer Systeme, Nöthnitzer Straße 38, 01187 Dresden, Germany*

(Dated: June 15, 2018)

For the paradigmatic frustrated spin-half Heisenberg antiferromagnet on the kagomé lattice we performed large-scale numerical investigation of thermodynamic functions by means of the finite-temperature Lanczos method for system sizes of up to $N = 42$. We present the dependence of magnetization as well as specific heat on temperature and external field and show in particular that a finite-size scaling of specific heat supports the appearance of a low-temperature shoulder below the major maximum. This seems to be the result of a counterintuitive motion of the density of singlet states towards higher energies. Other interesting features that we discuss are the asymmetric melting of the $1/3$ magnetization plateau as well the field dependence of the specific heat that exhibits characteristic features caused by the existence of a flat one-magnon band. By comparison with the unfrustrated square-lattice antiferromagnet the tremendous role of frustration in a wide temperature range is illustrated.

PACS numbers: 75.10.Jm, 75.50.Xx, 75.40.Mg

I. INTRODUCTION

The spin-1/2 kagomé Heisenberg antiferromagnet (KHAF) is one of the most prominent and at the same time challenging spin models in the field of frustrated quantum magnetism. The first challenge concerns the nature of the ground state (GS), on which a plethora of studies exist, see, e.g., Refs. 1–27. Although consensus on the absence of magnetic long-range order (LRO) is achieved, the precise nature of the spin-liquid GS, with quantum spin liquids and Dirac spin liquids as possible candidates,^{23,28} is not yet understood. Large-scale density matrix renormalization group (DMRG) and exact diagonalization (ED) studies^{13–15,22,23} suggest a tiny singlet-singlet gap $\Delta_s \sim (0.01 \dots 0.05)J$, where J denotes the exchange coupling in the Heisenberg model, and a sizeable singlet-triplet gap $\Delta_t \sim (0.13 \dots 0.17)J$. However, a very recent DMRG study using adiabatic flux insertion provides indications for a much smaller spin-gap in agreement with variational and other numerical techniques.^{12,17,23,24,26} The very existence of a gap is determinative for thermodynamics at low temperatures T . In addition, a triplet gap leads to an exponentially activated low-temperature behavior of the susceptibility. On the other hand, indications were found that a huge number of singlet states below the first triplet state may exist,^{2,3,7,13,14,16,22,29} being relevant for the specific heat C at low temperatures.

Besides the theoretical work there is also large activity on the experimental side, see, e.g., Refs. 30–46 and in particular the review 28. Among the spin-1/2 kagomé compounds, Herbertsmithite $\text{ZnCu}_3(\text{OH})_6\text{Cl}_2$ seems to be a promising candidate for a spin liquid.^{28,35–39,41,46,47}

The second challenge concerns the thermodynamic properties of the quantum KHAF on which far less studies exist.^{4,5,26,29,48–59} While systematic high-temperature

approaches^{48,53,54,56} provide reliable insight into the temperature dependence of physical quantities down to temperatures T of about 40% of the exchange coupling J , a reliable picture of the temperature dependences at $0 \leq T \lesssim 0.4J$ is still missing. Various methods^{48–51,55,57,58} provide indications for an additional low-temperature peak of the specific heat signaling an extra low-energy scale set by low-lying singlets. However, instead of a true maximum a shoulder-like hump may characterize the low- T profile of $C(T)$.^{26,51} Thus, the low- T behavior of the specific heat is another issue (in some relation to the gaps) that is not yet settled.

The third challenge is given by the magnetization process of the spin-1/2 KHAF.^{26,27,60–68} A series of magnetization plateaus at $3/9 (= 1/3)$, $5/9$ and $7/9$ of the saturation is found,^{26,65,66} among which the $1/3$ -plateau, already found by Hida,⁶⁰ is the widest. In addition to the above mentioned plateaus, there might be a tiny plateau at $1/9$.^{26,65} The magnetic ordering within the plateau is well-described by valence-bond states, i.e., the plateau states are of quantum nature.^{63,65,66} Moreover, there is a macroscopic jump to saturation related to the existence of a huge manifold of localized multi-magnon states.^{61,69–71} At low enough temperatures and for specific values of the magnetic field the plateaus as well as the magnetization jump are well expressed features of the magnetization curve. From the experimental point of view the detection of these features at low temperatures provides *smoking gun* evidence of the proximity of the investigated magnetic kagomé compound to the ideal KHAF model.

In the present paper we discuss the thermodynamic properties of the spin-1/2 KHAF on a finite lattice of $N = 42$ sites. These results were obtained by large-scale numerical calculations (5 Mio. core hours) using the finite-temperature Lanczos method (FTLM).^{72–76} The

extension to a lattice of this size yields an improved insight into the low-temperature physics of the model compared to previous ED and FTLM studies restricted to significantly smaller lattices.

The paper is organized as follow. In Section II we introduce the model and our numerical scheme. Thereafter in Section III we present our results for the KHAF followed by a discussion in Section IV.

II. HAMILTONIAN AND CALCULATIONAL SCHEME

The investigated spin systems are modeled by a spin-1/2 Heisenberg Hamiltonian augmented with a Zeeman term, i. e.

$$\tilde{H} = J \sum_{\langle i,j \rangle} \tilde{\vec{s}}_i \cdot \tilde{\vec{s}}_j + g\mu_B B \sum_i \tilde{s}_i^z. \quad (1)$$

Quantum mechanical operators are marked by a tilde. In what follows we set the antiferromagnetic nearest-neighbor exchange coupling to $J = 1$. The complete eigenvalue spectrum of a spin system composed of spins $s = 1/2$ can be evaluated for sizes of up to about $N = 24$ depending on the available symmetries.⁷⁷ The resulting thermodynamic quantities are then numerically exact.

For larger systems with Hilbert space dimensions of up to 10^{10} FTLM provides approximations of thermodynamic functions with astonishing accuracy.^{74–76} FTLM approximates the partition function in two ways:^{72,73}

$$Z(T, B) \approx \sum_{\gamma=1}^{\Gamma} \frac{\dim(\mathcal{H}(\gamma))}{R} \sum_{\nu=1}^R \sum_{n=1}^{N_L} e^{-\beta \epsilon_n^{(\nu)}} |\langle n(\nu) | \nu \rangle|^2. \quad (2)$$

The trace, i.e., the sum over an orthonormal basis, is in a Monte-Carlo fashion replaced by a much smaller sum over R random vectors $|\nu\rangle$ for each symmetry-related orthogonal subspace $\mathcal{H}(\gamma)$ of the Hilbert space. The exponential of the Hamiltonian is then approximated by its spectral representation in a Krylov space spanned by the N_L Lanczos vectors starting from the respective random vector $|\nu\rangle$. $|n(\nu)\rangle$ is the n -th eigenvector of \tilde{H} in this Krylov space. This allows to evaluate typical observables such as magnetization and specific heat.⁷⁸

The method was implemented in two independently self-written programs, one of which – `spinpack` – is publicly available.⁷⁹ The latter employs several symmetries in order to decompose the full Hilbert space into much smaller orthogonal subspaces according to the irreducible representations of the used symmetries. In our case \tilde{S}^z symmetry was used together with the longest cyclic point group (length 14 for $N = 42$) as well as with spin-flip-symmetry and a second commuting point group where applicable. The largest Hilbert sub-spaces in the sector with magnetic quantum number $M = 1$ assumed a dimension of $3.67 \cdot 10^{10}$. We used $R = 10$ in all subspaces of $M = 0$, i.e., for the subspaces that contain

the ground state and the lowest energy levels, $R = 4$ for $M = 1$, $R = 2$ for $M = 2, \dots, 8$ and then again $R = 10$ for $8 < M < 16$. The number of Lanczos iterations for each random vector was determined by reaching convergence for the two lowest energy levels. In subspaces with $M \geq 16$ the Hamiltonian was diagonalized completely. The total computation time for the kagomé system of 42 sites was $\sim 5 \cdot 10^6$ core hours at the Leibniz Supercomputing Center's `supermuc`.

III. KAGOMÉ LATTICE ANTIFERROMAGNET $N = 42$

In what follows we focus on the specific heat, the density of states, the uniform susceptibility, the entropy and the magnetization process.

A. Zero-field properties

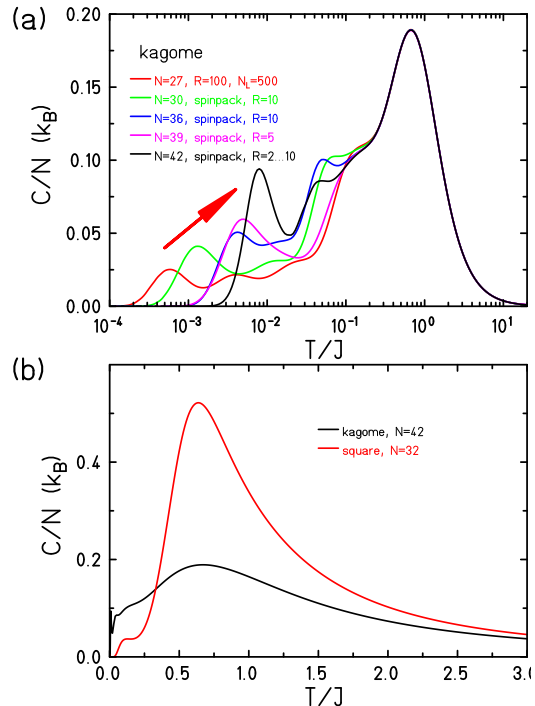


Figure 1. (Color online) (a) Specific heat of the KHAF as function of temperature at $B = 0$ for various systems sizes (logarithmic temperature scale). (b) Specific heat of the KHAF and the SHAF as function of temperature at $B = 0$ (linear temperature scale).

We start with the discussion of the specific heat $C(T)$, the entropy $S(T)$ and the uniform susceptibility $\chi_0(T)$ using a logarithmic scale for T in order to make the low-temperature features transparent, see Figs. 1(a), 3(a), and 4(a). The main maximum in the specific heat, set by the exchange J , is at $T = 0.67$, its height is

$C(T = 0.67)/N = 0.189$.⁸⁰ Below $T = 0.25$ the curvature of $C(T)$ changes and a shoulder-like profile is present for $0.1 < T < 0.25$. This feature seems to be size-independent, i.e., finite-size effects appear likely only at $T < 0.1$. In this low-temperature region also a difference between odd and even lattice sizes N occurs, that is related to the GS value of the total spin (doublet vs singlet), where even N with a singlet GS seem to better fit to the spin-liquid GS present for thermodynamically large systems.

The behavior at very low temperatures $T < 0.1$ deserves a specific discussion, where we focus on even $N = 30, 36$ and 42 . First we notice that for $N = 36$ and 42 just below the shoulder there is a rather flat maximum at about $T = 0.05$. At very low temperatures we observe a well pronounced extra peak in the specific heat. This peak marks the appearance of low-lying singlets above the ground state and is thus related to the singlet-singlet gap. Common expectations are that such gaps shrink with increasing size N . But in accordance with recent exact diagonalization studies,²² this peak moves towards higher temperatures with increasing N , as highlighted by the arrow in Fig. 1(a). One reason is that the singlet-singlet gap as well as the singlet-triplet gap do not shrink (considerably) when going from $N = 36$ to $N = 42$ and even $N = 48$, instead the singlet-singlet gap grows and the singlet-triplet gap shrinks only slightly.²² This behavior can be further rationalized by looking at the total density of states $n(E^*)$ as a function of the respective excitation energy E^* and the contributions of the different sectors of total magnetization M to $n(E^*)$ as displayed in Fig. 2. The density of states is evaluated by histogramming the Krylov space energy eigenvalues together with their respective weights. The bin size is chosen as $J/100$. From Fig. 2 it becomes obvious which sector of M contributes to $C(T)/N$ at various low-temperature regimes.

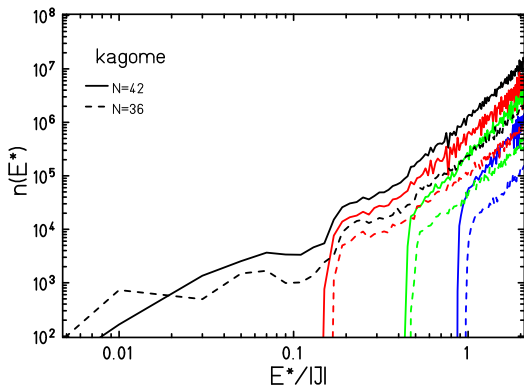


Figure 2. (Color online) Binned density of states for $N = 36$ (dashed curves) and $N = 42$ (solid curves) as a function of the respective excitation energy E^* : total density of states – black, total density of states for $|M| = 1$ – red, for $|M| = 2$ – green, and for $|M| = 3$ – blue.

Having in mind the sum rule

$$\int_0^\infty \frac{C(T)}{NT} dT = \int_{T=0}^{T=\infty} ds = s_\infty - s_0 = k_B \log(2), \quad (3)$$

we may speculate that the weight of the extra peak at very low temperatures moves towards the shoulder with increasing $N \rightarrow \infty$, thus making the shoulder more pronounced. To conclude, we argue that our results are in favor of a low-temperature shoulder rather than an additional low-temperature maximum, compare Fig. 1(b). This is in accordance with recent tensor network calculations.²⁶

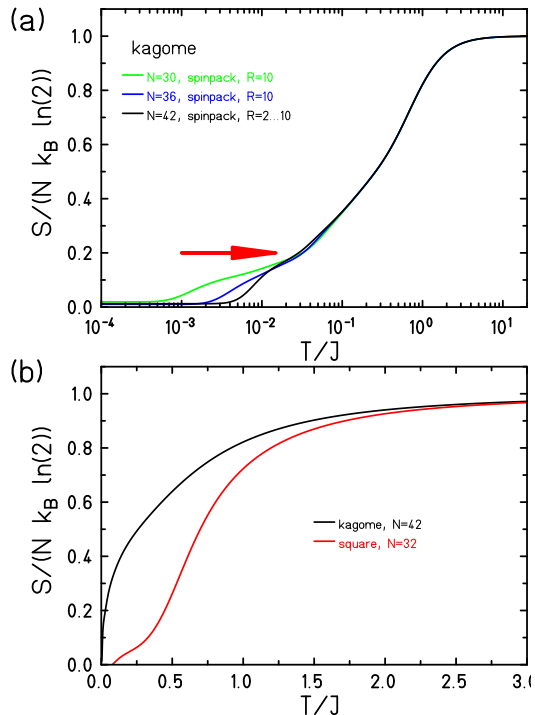


Figure 3. (Color online) (a) Entropy of the KHAF as function of temperature at $B = 0$ for various systems sizes (logarithmic temperature scale); the arrow marks the movement of the low-lying density of states. (b) Entropy of the KHAF and the SHAF as function of temperature at $B = 0$ (linear temperature scale).

The behavior of the low-temperature peak also means that concerning the density of singlet states, weight is not simply shifted towards lower and lower energies with increasing N . It may be that the singlet-singlet gap closes with increasing N , but the density profile seems to behave differently, as can be noted by comparing the dashed ($N = 36$) and solid black ($N = 42$) curves in Fig. 2. This observation is further supported by the behavior of the entropy $S(T)$ at $B = 0$, which is shown in Fig. 3. As highlighted by the arrow, the temperature above which the entropy rises moves towards higher temperatures with increasing N in accordance with the motion of the low-temperature maximum of $C(T)$.

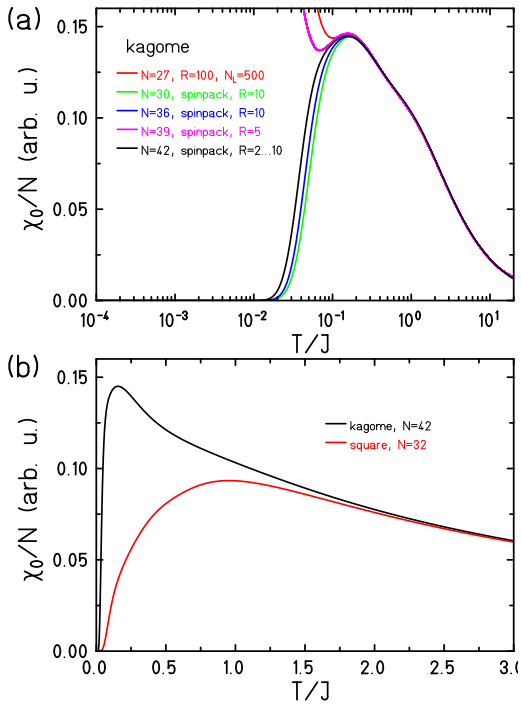


Figure 4. (Color online) (a) Susceptibility of the KHAF as function of temperature at $B = 0$ for various systems sizes (logarithmic temperature scale). (b) Susceptibility of the KHAF and the SHAF as function of temperature at $B = 0$ (linear temperature scale).

The singlet-triplet gap is even larger than the singlet-singlet gap, therefore the zero-field susceptibility exhibits a gapped behavior, as displayed in Fig. 4. For odd N the ground state possesses non-zero spin, therefore the susceptibility diverges Curie-like in these cases. Since the singlet-triplet gap does not move much with increasing size N , it is not possible to draw definite conclusions about the functional form of χ for $T \rightarrow 0$. Nevertheless, DMRG calculations suggest that the singlet-triplet gap does not vanish in the thermodynamic limit, but approaches $0.13(1)$.¹⁵

Finally, we compare $C(T)$, $S(T)$ and $\chi_0(T)$ for the (highly frustrated) KHAF with the corresponding FTLM data for the (unfrustrated) spin-1/2 square-lattice Heisenberg antiferromagnet (SHAF) of $N = 32$ sites, see Figs. 1 (b), 3 (b), and 4 (b), where we use a linear temperature scale. The temperature profile of all three quantities exhibits significant differences between the KHAF and the SHAF illustrating the tremendous role of frustration in a wide temperature range and, in particular, at low temperatures.⁸¹ Note that at high temperatures the quantities $C(T)$, $S(T)$ and $\chi_0(T)$ for both models approach each other, since square and kagomé lattices have identical coordination number $z = 4$. Thus the high-temperature series for C and χ_0 are identical up to order $1/T^2$ and $1/T^3$, respectively, see, e.g., Refs. 54 and 82.

B. Field-dependent properties

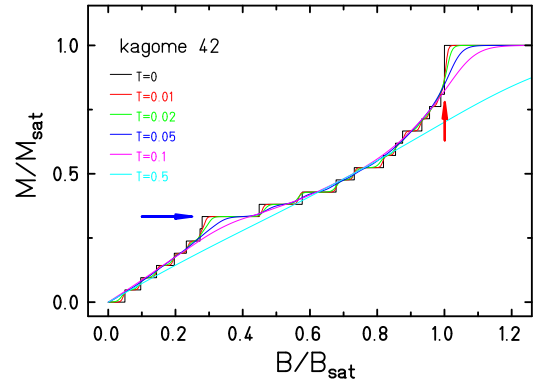


Figure 5. (Color online) Magnetization vs applied magnetic field for various temperatures: both magnetization and field are normalized by their saturation values.

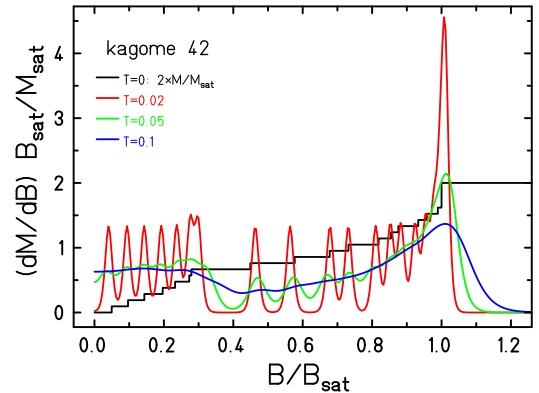


Figure 6. (Color online) Derivative dM/dB vs applied magnetic field B for various temperatures for $N = 42$. Both, magnetization and field are normalized by their saturation values.

The KHAF exhibits a number of interesting properties in an applied magnetic field.^{27,60–67,69,70} Magnetization plateaus exist at $3/9 (= 1/3)$, $5/9$ and $7/9$ of the saturation magnetization M_{sat} for the infinite system at $T = 0$, where the $1/3$ plateau is the widest. An additional tiny plateau at $1/9$ appears possible.⁶⁵ Moreover, the magnetization curve at $T = 0$ shows a macroscopic jump to saturation due to the existence of independent localized magnons.^{61,69–71,83}

In a calculation of a small lattice the magnetization curve is unavoidably a sequence of steps, that happen at ground state level crossings at certain field values, compare Fig. 5. Thus, due to this discretization the existence of smaller plateaus cannot be unambiguously deduced from such a single magnetization curve. Moreover, a specific plateau value $M_{\text{plateau}}/M_{\text{sat}}$ can be missed in the $M(B)$ curve, if it does not fit to the lattice size N . For example, for our largest system of $N = 42$ the val-

ues at $M_{\text{plateau}}/M_{\text{sat}} = 5/9$ and $7/9$ are not present in Fig. 5 – for $M(B)$ curves of other finite kagomé lattices, see, e.g., Refs. 27, 62, 66, and 67. Nevertheless, the major plateau at $1/3$ (marked by the blue horizontal arrow) is clearly visible in Fig. 5, since it is the widest of all plateaus and it is very robust as a function of N .^{61,62,66} The jump to saturation (marked by the red vertical arrow) does not suffer from finite-size effects. Its existence is analytically proven and persists for all sizes.^{61,83} We also mention that the pretty wide plateaus just above the $1/3$ -plateau most likely disappear for $N \rightarrow \infty$.⁶⁵ The influence of the temperature on the $M(B)$ curve is relevant for experimental studies. From Fig. 5 it is obvious that for slightly elevated temperatures the detection of plateaus by measuring $M(B)$ is difficult. Therefore, the first derivative dM/dB as a function of T as presented in Fig. 6 is often used in experiments to find plateaus, cf., e.g., Ref. 84. The $1/3$ -plateau can be detected by the pronounced minimum in dM/dB . Note that the oscillations of the red dM/dB curve are also due to finite-size effects. It is worth mentioning that the position of the minimum in dM/dB stemming from the $1/3$ -plateau is shifted to higher values of B with increasing temperature. Thus, for $T = 0.05$ ($T = 0.02$) it is at $B/B_{\text{sat}} = 0.398$ ($B/B_{\text{sat}} = 0.381$) whereas the midpoint of the plateau is at $B/B_{\text{sat}} = 0.364$. For $T = 0.1$ the minimum in dM/dB is hardly detectable, see Fig. 6. This shift is related to the ‘asymmetric melting’ of the plateau due to the larger density of low-lying excited states below the plateau than that of low-lying excitations above the plateau.⁵⁸ Thus, for the KHAF the very existence of the plateau can be found by measuring dM/dB at $T \lesssim 0.1$, but to determine the precise position of it requires very low temperatures. Last but not least, we notice that the jump of the magnetization to saturation at $T = 0$ is washed out at $T > 0$, but its existence leads to a high peak in dM/dB at the saturation field.

The influence of the magnetic field B on the specific heat C is shown in Fig. 7 for $N = 42$. At very low temperatures and moderate fields the influence of B is determined by the shift of the low-lying magnetic excitations with $M = 1$ and $M = 2$ towards and even beyond the zero-field singlet GS. As a result, the position and the height of the low-temperature (finite-size) peaks in $C(T)$ are substantially changed. At temperatures below the main maximum there is no obvious systematic behavior of $C(T)$ as a function of B , see Fig. 7(a). However, at magnetic fields slightly below and above the saturation field, the huge manifold of low-lying localized multimagnon states (already mentioned in the introduction) leads to an extra low-temperature maximum, see Fig. 7(b), persisting in the thermodynamic limit.^{61,70,71,85} It is worth mentioning, that for $B \lesssim B_{\text{sat}}$ in the thermodynamic limit this extra-maximum likely becomes a true singularity indicating a low-temperature order-disorder transition into a magnon-crystal phase.^{70,86}

Interestingly, the influence of B on the main maxi-

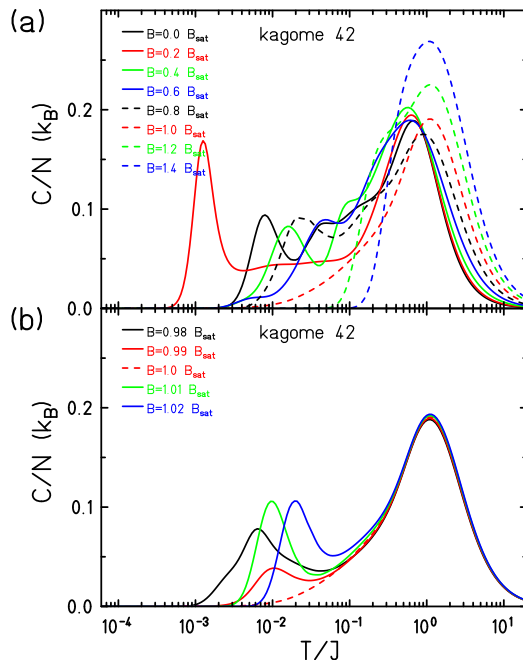


Figure 7. (Color online) Specific heat of the KHAF as function of temperature for several values of the magnetic field varying from $B = 0$ to $B = 1.4B_{\text{sat}}$ (a) and for magnetic-field values at and close to the saturation field B_{sat} (b).

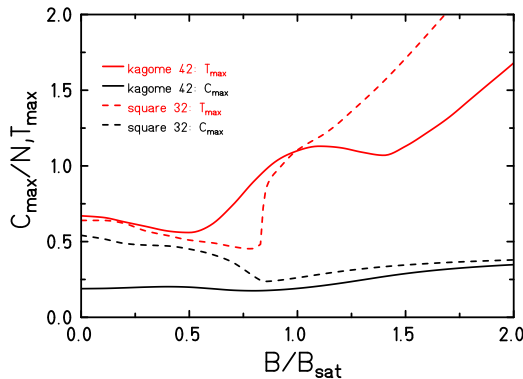


Figure 8. (Color online) Position of the maximum in $C(T)$ in dependence of the magnetic field B .

imum of C depicted in Fig. 8 shows some systematics (see also Ref. 26, Fig. 3): (i) The height of the maximum C_{max} remains almost constant until $B \sim 0.8B_{\text{sat}}$ and increases smoothly for $B > B_{\text{sat}}$. (ii) The position of the maximum T_{max} as a function of B exhibits two maxima at $B = 0$ and $B \approx 1.1B_{\text{sat}}$ and two minima at $B \approx 0.5B_{\text{sat}}$ and $B \approx 1.4B_{\text{sat}}$ as well as two regions $0.65B_{\text{sat}} \lesssim B \lesssim 0.9B_{\text{sat}}$ and $B \gtrsim 1.5B_{\text{sat}}$ with an (almost) linear growth of T_{max} . To illuminate the role of frustration we contrast this behavior with that of the unfrustrated SHAF, also see Fig. 8. At low magnetic fields the value of T_{max} is determined by J , and for both models T_{max} behaves very similar. On the other hand, the difference in C_{max} is significant and can be related to the

different low-energy physics which influences C at higher T according to the sum rule (3). Beyond $B \sim 0.5B_{\text{sat}}$ the different behavior is more evident. The almost straight increase in $T_{\text{max}}(B)$ for $0.65B_{\text{sat}} \lesssim B \lesssim 0.9B_{\text{sat}}$ in the case of the KHAF indicates a paramagnetic behavior. The maximum around $B = B_{\text{sat}}$ signals strong frustration because it is related to the manifold \mathcal{W} of localized multi-magnon states setting an extra low-energy scale in the vicinity of the saturation field in frustrated Heisenberg systems with a flat band. For the specific flat-band model under consideration, i.e., the KHAF, the number of localized multimagnon states grows exponentially with system size as $\mathcal{W} \sim e^{0.111081N}$ and is thus relevant for the behavior of the specific heat.^{69,70} The linear increase of T_{max} above B_{sat} present in both models is then related to the paramagnetic phase. Note, however, that this linear behavior starts at much higher fields for the KHAF. We may therefore conclude, that flat-band spin physics, that is typically relevant at low-energy scales $T \ll J$, is observable in the dependence of the specific heat on magnetic field even at pretty high temperatures of $T \sim J$.

IV. DISCUSSION

What is the gain of our new calculation for a KHAF with now $N = 42$ sites?

First of all, it is by far the largest calculation of thermodynamic properties such as magnetization and specific heat. Other calculations such as Lanczos diagonalization for $N = 48$ as well as DMRG calculations aim at ground state properties and at some low-lying states. Our results for $N = 42$ and smaller sizes reveal that the specific heat very likely has got a low-temperature shoulder instead of an additional low-temperature maximum.

As a second result we can show that ‘asymmetric melting’ of the 1/3-plateau indeed occurs. Asymmetric melting influences our ability to determine the plateau in measurements of dM/dB . We further speculate that in addition to a non-balanced density of states at the endpoints of the plateau the overall magnitude of the density of states grows with the size N of the lattice. This would mean that one would need increasingly low temperatures in order to accurately measure the 1/3-plateau.^{67,87}

Further, we found that effects of strong frustration

are not only visible at low temperatures $T \ll J$, they are clearly visible at moderate (and high) temperatures $T \sim J$. In particular, the very existence of a flat one-magnon band yielding a huge manifold of low-lying localized multi-magnon states leads to pronounced effects in the magnetization curve and the temperature profile of the specific heat at magnetic fields near saturation.

In accordance with Ref. 22 we also found that in the low-field regime the convergence at $T \lesssim 0.1J$ to the thermodynamic limit is slow. Both the singlet-singlet gap as well as the singlet-triplet gap change very little with increasing system size. Therefore, at $B = 0$ the behavior below $T \lesssim 0.1J$ seen in our calculations is still dominated by finite-size effects.

Finally, we mention that the relation of our data to the experimental data of the spin-liquid candidate Herbertsmithite^{35–39,41,47} is limited for several reasons. First, the exchange interaction of this compound is estimated as $J = 190$ K. Low-temperature measurements of the magnetization as well as the specific heat, in particular for $2\text{K} \leq T \leq 10\text{K}$, are well below $0.1J$ and can thus, unfortunately, not be compared with our simulations due to the finite-size effects below $0.1J$. Second, it is up to now not settled how the interacting impurities as well as the lattice vacancies in Herbertsmithite can be dealt with in thermodynamic calculations.^{45,88} Moreover, there might be a noticeable spin anisotropy present in Herbertsmithite. Despite all the uncertainties, it is believed that the spin liquid ground state is a rather stable phenomenon.^{45,88–91}

In view of the numerical effort of our investigations we conjecture that exact diagonalization studies of the thermodynamic behavior of the KHAF might be feasible for $N = 45$ and $N = 48$,²² but larger systems must be dealt with by, e.g., DMRG and tensor network methods.^{23,26}

ACKNOWLEDGMENT

This work was supported by the Deutsche Forschungsgemeinschaft (DFG SCHN 615/23-1). Computing time at the Leibniz Center in Garching is gratefully acknowledged. JR is indebted to O.Derzhko for valuable discussions.

* jschnack@uni-bielefeld.de

† Johannes.Richter@physik.uni-magdeburg.de

¹ C. Zeng and V. Elser, “Numerical studies of antiferromagnetism on a kagomé net,” *Phys. Rev. B* **42**, 8436–8444 (1990).

² C. Waldtmann, H.-U. Everts, B. Bernu, C. Lhuillier, P. Sindzingre, P. Lecheminant, and L. Pierre, “First excitations of the spin 1/2 Heisenberg antiferromagnet on the kagomé lattice,” *EPJB* **2**, 501–507 (1998).

³ P. Azaria, C. Hooley, P. Lecheminant, C. Lhuillier, and A. M. Tsvelik, “Kagomé lattice antiferromagnet stripped to its basics,” *Phys. Rev. Lett.* **81**, 1694–1697 (1998).

⁴ W. Yu and S. Feng, “Spin-liquid state for two-dimensional Heisenberg antiferromagnets on a kagomé lattice,” *EPJB* **13**, 265–269 (2000).

⁵ B. H. Bernhard, B. Canals, and C. Lacroix, “Green’s function approach to the magnetic properties of the kagomé antiferromagnet,” *Phys. Rev. B* **66**, 104424 (2002).

- ⁶ R. R. P. Singh and D. A. Huse, “Ground state of the spin-1/2 kagome-lattice Heisenberg antiferromagnet,” *Phys. Rev. B* **76**, 180407 (2007).
- ⁷ H. C. Jiang, Z. Y. Weng, and D. N. Sheng, “Density matrix renormalization group numerical study of the kagome antiferromagnet,” *Phys. Rev. Lett.* **101**, 117203 (2008).
- ⁸ A. M. Läuchli and C. Lhuillier, “Dynamical correlations of the kagome $S = 1/2$ Heisenberg quantum antiferromagnet,” ArXiv e-prints (2009), [arXiv:0901.1065 \[cond-mat.str-el\]](https://arxiv.org/abs/0901.1065).
- ⁹ G. Evenbly and G. Vidal, “Frustrated antiferromagnets with entanglement renormalization: Ground state of the spin-1/2 Heisenberg model on a kagome lattice,” *Phys. Rev. Lett.* **104**, 187203 (2010).
- ¹⁰ O. Götze, D. J. J. Farnell, R. F. Bishop, P. H. Y. Li, and J. Richter, “Heisenberg antiferromagnet on the kagome lattice with arbitrary spin: A higher-order coupled cluster treatment,” *Phys. Rev. B* **84**, 224428 (2011).
- ¹¹ H. Nakano and T. Sakai, “Numerical-diagonalization study of spin gap issue of the kagome lattice Heisenberg antiferromagnet,” *J. Phys. Soc. Jpn.* **80**, 053704 (2011).
- ¹² Y. Iqbal, F. Becca, and D. Poilblanc, “Projected wave function study of z_2 spin liquids on the kagome lattice for the spin-1/2 quantum Heisenberg antiferromagnet,” *Phys. Rev. B* **84**, 020407 (2011).
- ¹³ S. Yan, D. A. Huse, and S. R. White, “Spin-liquid ground state of the $s = 1/2$ Kagome Heisenberg antiferromagnet,” *Science* **332**, 1173–1176 (2011).
- ¹⁴ A. M. Läuchli, J. Sudan, and E. S. Sørensen, “Ground-state energy and spin gap of spin-1/2 kagomé-Heisenberg antiferromagnetic clusters: Large-scale exact diagonalization results,” *Phys. Rev. B* **83**, 212401 (2011).
- ¹⁵ Stefan Depenbrock, Ian P. McCulloch, and Ulrich Schollwöck, “Nature of the spin-liquid ground state of the $s = 1/2$ Heisenberg model on the kagome lattice,” *Phys. Rev. Lett.* **109**, 067201 (2012).
- ¹⁶ I. Rousochatzakis, R. Moessner, and J. v. d. Brink, “Frustrated magnetism and resonating valence bond physics in two-dimensional kagome-like magnets,” *Phys. Rev. B* **88**, 195109 (2013).
- ¹⁷ Yasir Iqbal, Federico Becca, Sandro Sorella, and Didier Poilblanc, “Gapless spin-liquid phase in the kagome spin- $\frac{1}{2}$ Heisenberg antiferromagnet,” *Phys. Rev. B* **87**, 060405 (2013).
- ¹⁸ I. Rousochatzakis, Y. Wan, O. Tchernyshyov, and F. Mila, “Quantum dimer model for the spin-1/2 kagome Z_2 spin liquid,” *Phys. Rev. B* **90**, 100406 (2014).
- ¹⁹ Z. Y. Xie, J. Chen, J. F. Yu, X. Kong, B. Normand, and T. Xiang, “Tensor renormalization of quantum many-body systems using projected entangled simplex states,” *Phys. Rev. X* **4**, 011025 (2014).
- ²⁰ F. Kolley, S. Depenbrock, I. P. McCulloch, U. Schollwöck, and V. Alba, “Phase diagram of the $J_1 - J_2$ Heisenberg model on the kagome lattice,” *Phys. Rev. B* **91**, 104418 (2015).
- ²¹ O. Götze and J. Richter, “Ground-state phase diagram of the XXZ spin- s kagome antiferromagnet: A coupled-cluster study,” *Phys. Rev. B* **91**, 104402 (2015).
- ²² A. M. Läuchli, J. Sudan, and R. Moessner, “The kagome $S = 1/2$ Heisenberg antiferromagnet revisited,” ArXiv e-prints (2016), [arXiv:1611.06990 \[cond-mat.str-el\]](https://arxiv.org/abs/1611.06990).
- ²³ Y.C. He, M. P. Zaletel, M. Oshikawa, and F. Pollmann, “Signatures of Dirac cones in a DMRG study of the kagome Heisenberg model,” *Phys. Rev. X* **7**, 031020 (2017).
- ²⁴ H. J. Liao, Z. Y. Xie, J. Chen, Z. Y. Liu, H. D. Xie, R. Z. Huang, B. Normand, and T. Xiang, “Gapless spin-liquid ground state in the $s=1/2$ kagome antiferromagnet,” *Phys. Rev. Lett.* **118**, 137202 (2017).
- ²⁵ Jia-Wei Mei, Ji-Yao Chen, Huan He, and Xiao-Gang Wen, “Gapped spin liquid with \mathbb{Z}_2 topological order for the kagome Heisenberg model,” *Phys. Rev. B* **95**, 235107 (2017).
- ²⁶ X. Chen, S.-J. Ran, T. Liu, C. Peng, Y.-Z. Huang, and G. Su, “Finite-temperature phase diagram and algebraic paramagnetic liquid in the spin-1/2 kagome Heisenberg antiferromagnet,” ArXiv e-prints (2017), [arXiv:1711.01001 \[cond-mat.str-el\]](https://arxiv.org/abs/1711.01001).
- ²⁷ Hiroki Nakano and Toru Sakai, “Numerical-diagonalization study of magnetization process of frustrated spin-1/2 Heisenberg antiferromagnets in two dimensions: Triangular- and kagome-lattice antiferromagnets,” *J. Phys. Soc. Jpn.* **87**, 063706 (2018).
- ²⁸ M. R. Norman, “Colloquium: Herbertsmithite and the search for the quantum spin liquid,” *Rev. Mod. Phys.* **88**, 041002 (2016).
- ²⁹ P. Sindzingre, G. Misguich, C. Lhuillier, B. Bernu, L. Pierce, C. Waldtmann, and H. U. Everts, “Magnetothermodynamics of the spin-1/2 kagome antiferromagnet,” *Phys. Rev. Lett.* **84**, 2953–2956 (2000).
- ³⁰ J. L. Atwood, “Kagome lattice - a molecular toolkit for magnetism,” *Nat. Mater.* **1**, 91–92 (2002).
- ³¹ Takashi Kambe, Yoshio Nogami, Kokichi Oshima, Wataru Fujita, and Kunio Awaga, “Structural phase transition in two-dimensional kagomé antiferromagnet m - N -methylpyridinium α -nitronyl nitroxide- $\text{BF}_4 \cdot \frac{1}{3}$ (acetone),” *J. Phys. Soc. Jpn.* **73**, 796–799 (2004).
- ³² J. S. Helton, K. Matan, M. P. Shores, E. A. Nytko, B. M. Bartlett, Y. Qiu, D. G. Nocera, and Y. S. Lee, “Dynamic scaling in the susceptibility of the spin- $\frac{1}{2}$ kagome lattice antiferromagnet herbertsmithite,” *Phys. Rev. Lett.* **104**, 147201 (2010).
- ³³ Sandra A. Reisinger, Chiu C. Tang, Stephen P. Thompson, Finlay D. Morrison, and Philip Lightfoot, “Structural phase transition in the $s = 1/2$ kagome system $\text{Cs}_2\text{ZrCu}_3\text{F}_{12}$ and a comparison to the valence-bond-solid phase in $\text{Rb}_2\text{SnCu}_3\text{F}_{12}$,” *Chem. Mater.* **23**, 4234–4240 (2011).
- ³⁴ Hiroyuki Yoshida, Yuichi Michiue, Eiji Takayama-Muromachi, and Masaaki Isobe, “ β -Vesignieite $\text{BaCu}_3\text{V}_2\text{O}_8(\text{OH})_2$: a structurally perfect $s = 1/2$ kagome antiferromagnet,” *J. Mater. Chem.* **22**, 18793–18796 (2012).
- ³⁵ P. Mendels, F. Bert, M. A. de Vries, A. Olariu, A. Harrison, F. Duc, J. C. Trombe, J. S. Lord, A. Amato, and C. Baines, “Quantum magnetism in the paratacamite family: Towards an ideal kagomé lattice,” *Phys. Rev. Lett.* **98**, 077204 (2007).
- ³⁶ J. S. Helton, K. Matan, M. P. Shores, E. A. Nytko, B. M. Bartlett, Y. Yoshida, Y. Takano, A. Suslov, Y. Qiu, J.-H. Chung, D. G. Nocera, and Y. S. Lee, “Spin Dynamics of the Spin-1/2 Kagome Lattice Antiferromagnet- $\text{ZnCu}_3(\text{OH})_6\text{Cl}_2$,” *Phys. Rev. Lett.* **98**, 107204 (2007).
- ³⁷ Z. Hiroi, H. Yoshida, Y. Okamoto, and M. Takigawa, “Spin-1/2 kagome compounds: Volborthite vs herbertsmithite,” *J. Phys.: Conf. Ser.* **145**, 012002 (2009).
- ³⁸ M. A. de Vries, J. R. Stewart, P. P. Deen, J. O. Piatek, G. J. Nilsen, H. M. Rønnow, and A. Harrison, “Scale-free antiferromagnetic fluctuations in the $s=1/2$ kagome

- antiferromagnet herbertsmithite,” *Phys. Rev. Lett.* **103**, 237201 (2009).
- ³⁹ D. Wulferding, P. Lemmens, P. Scheib, J. Röder, P. Mendels, S. Chu, T. Han, and Y. S. Lee, “Interplay of thermal and quantum spin fluctuations in the kagome lattice compound herbertsmithite,” *Phys. Rev. B* **82**, 144412 (2010).
- ⁴⁰ Farida H. Aidoudi, David W. Aldous, Richard J. Goff, Alexandra M. Z. Slawin, J. Paul Attfield, Russell E. Morris, and Philip Lightfoot, “An ionothermally prepared $s = 1/2$ vanadium oxyfluoride kagome lattice,” *Nat. Chem.* **3**, 801–806 (2011).
- ⁴¹ T.-H. Han, J. S. Helton, S. Chu, D. G. Nocera, J. A. Rodriguez-Rivera, C. Broholm, and Y. S. Lee, “Fractionalized excitations in the spin-liquid state of a kagome-lattice antiferromagnet,” *Nature* **492**, 406–410 (2012).
- ⁴² Mingxuan Fu, Takashi Imai, Tian-Heng Han, and Young S. Lee, “Evidence for a gapped spin-liquid ground state in a kagome Heisenberg antiferromagnet,” *Science* **350**, 655–658 (2015).
- ⁴³ Zili Feng, Zheng Liand, Xin Meng, Wei Yi, Yuan Wei, Jun Zhang, Yan-Cheng Wang, Wei Jiang, Zheng Liu, Shiyang Li, Feng Liu, Jianlin Luo, Shiliang Li, Guo qing Zheng, Zi Yang Meng, Jia-Wei Mei, and Youguo Shi, “Gapped spin-1/2 spinon excitations in a new kagome quantum spin liquid compound $\text{Cu}_3\text{Zn}(\text{OH})_6\text{FBr}$,” *Chinese Physics Letters* **34**, 077502 (2017).
- ⁴⁴ M. Gomilšek, M. Klanjšek, R. Žitko, M. Pregelj, F. Bert, P. Mendels, Y. Li, Q. M. Zhang, and A. Zorko, “Field-induced instability of a gapless spin liquid with a spinon fermi surface,” *Phys. Rev. Lett.* **119**, 137205 (2017).
- ⁴⁵ J.-C. Orain, B. Bernu, P. Mendels, L. Clark, F. H. Aidoudi, P. Lightfoot, R. E. Morris, and F. Bert, “Nature of the spin liquid ground state in a breathing kagome compound studied by nmr and series expansion,” *Phys. Rev. Lett.* **118**, 237203 (2017).
- ⁴⁶ A. Zorko, M. Herak, M. Gomilšek, J. van Tol, M. Velázquez, P. Khuntia, F. Bert, and P. Mendels, “Symmetry reduction in the quantum kagome antiferromagnet herbertsmithite,” *Phys. Rev. Lett.* **118**, 017202 (2017).
- ⁴⁷ R. Chisnell, J. S. Helton, D. E. Freedman, D. K. Singh, R. I. Bewley, D. G. Nocera, and Y. S. Lee, “Topological magnon bands in a kagome lattice ferromagnet,” *Phys. Rev. Lett.* **115**, 147201 (2015).
- ⁴⁸ N. Elstner and A. P. Young, “Spin-1/2 Heisenberg antiferromagnet on the kagome lattice: High-temperature expansion and exact-diagonalization studies,” *Phys. Rev. B* **50**, 6871–6876 (1994).
- ⁴⁹ Tota Nakamura and Seiji Miyashita, “Thermodynamic properties of the quantum Heisenberg antiferromagnet on the kagomé lattice,” *Phys. Rev. B* **52**, 9174–9177 (1995).
- ⁵⁰ Piotr Tomczak and Johannes Richter, “Thermodynamical properties of the Heisenberg antiferromagnet on the kagomé lattice,” *Phys. Rev. B* **54**, 9004–9006 (1996).
- ⁵¹ G. Misguich and B. Bernu, “Specific heat of the $s = \frac{1}{2}$ Heisenberg model on the kagome lattice: High-temperature series expansion analysis,” *Phys. Rev. B* **71**, 014417 (2005).
- ⁵² G. Misguich and P. Sindzingre, “Magnetic susceptibility and specific heat of the spin-1/2 Heisenberg model on the kagome lattice and experimental data on $\text{zncu}_3(\text{oh})_6\text{cl}_2$,” *Eur. Phys. J B* **59**, 305–309 (2007).
- ⁵³ Marcos Rigol, Tyler Bryant, and Rajiv R. P. Singh, “Numerical linked-cluster algorithms. I. spin systems on square, triangular, and kagomé lattices,” *Phys. Rev. E* **75**, 061118 (2007).
- ⁵⁴ A. Lohmann, H.-J. Schmidt, and J. Richter, “Tenth-order high-temperature expansion for the susceptibility and the specific heat of spin- s Heisenberg models with arbitrary exchange patterns: Application to pyrochlore and kagome magnets,” *Phys. Rev. B* **89**, 014415 (2014).
- ⁵⁵ Tomu Munehisa, “An improved finite temperature lanczos method and its application to the spin-1/2 Heisenberg model on the kagome lattice,” *World Journal of Condensed Matter Physics* **4**, 134–140 (2014).
- ⁵⁶ N. E. Sherman P. and R. R. P. Singh, “Structure factors of the kagome-lattice Heisenberg antiferromagnets at finite temperatures,” ArXiv e-prints (2017), arXiv:1711.053375 [cond-mat.str-el].
- ⁵⁷ T. Shimokawa and H. Kawamura, “Finite-temperature crossover phenomenon in the $s=1/2$ antiferromagnetic Heisenberg model on the kagome lattice,” *J. Phys. Soc. Jpn.* **85**, 113702 (2016).
- ⁵⁸ T. Misawa, Y. Motoyama, and Y. Yamaji, “Asymmetric melting of one-third plateau in kagome quantum antiferromagnets,” ArXiv e-prints (2018), arXiv:1801.07128 [cond-mat.str-el].
- ⁵⁹ P. Müller, A. Zander, and J. Richter, “Thermodynamics of the kagome-lattice Heisenberg antiferromagnet with arbitrary spin s ,” ArXiv e-prints (2018), arXiv:1803.06202 [cond-mat.str-el].
- ⁶⁰ Kazuo Hida, “Magnetization process of the $s=1$ and $1/2$ uniform and distorted kagome Heisenberg antiferromagnets,” *J. Phys. Soc. Jpn.* **70**, 3673 (2001).
- ⁶¹ Jörg Schulenburg, Andreas Honecker, Jürgen Schnack, Johannes Richter, and Heinz-Jürgen Schmidt, “Macroscopic magnetization jumps due to independent magnons in frustrated quantum spin lattices,” *Phys. Rev. Lett.* **88**, 167207 (2002).
- ⁶² Andreas Honecker, Jörg Schulenburg, and Johannes Richter, “Magnetization plateaus in frustrated antiferromagnetic quantum spin models,” *J. Phys.: Condens. Matter* **16**, S749 (2004).
- ⁶³ Andreas Honecker, D.C.Cabra, M.D. Grynberg, P.C.W. Holdsworth, P. Pujol, Johannes Richter, D. Schmalfluss, and J. Schulenburg, “Ground state and low-lying excitations of the spin-1/2 XXZ model on the kagome lattice at magnetization $1/3$,” *Physica B* **359**, 1391–1393 (2005).
- ⁶⁴ Tōru Sakai and Hiroki Nakano, “Critical magnetization behavior of the triangular- and kagome-lattice quantum antiferromagnets,” *Phys. Rev. B* **83**, 100405 (2011).
- ⁶⁵ S. Nishimoto, N. Shibata, and C. Hotta, “Controlling frustrated liquids and solids with an applied field in a kagome Heisenberg antiferromagnet,” *Nature Com.* **4**, 2287 (2013).
- ⁶⁶ Sylvain Capponi, Oleg Derzhko, Andreas Honecker, Andreas M. Läuchli, and Johannes Richter, “Numerical study of magnetization plateaus in the spin- $\frac{1}{2}$ kagome Heisenberg antiferromagnet,” *Phys. Rev. B* **88**, 144416 (2013).
- ⁶⁷ Hiroki Nakano and Tōru Sakai, “Anomalous behavior of the magnetization process of the $s = 1/2$ kagome-lattice Heisenberg antiferromagnet at one-third height of the saturation,” *J. Phys. Soc. Jpn.* **83**, 104710 (2014), <https://doi.org/10.7566/JPSJ.83.104710>.
- ⁶⁸ Xavier Plat, Tsutomu Momoi, and Chisa Hotta, “Kinetic frustration induced supersolid in the $s=1/2$ kagome lattice antiferromagnet in a magnetic field,” ArXiv e-prints (2018), arXiv:1804.00789 [cond-mat.str-el].

- ⁶⁹ Oleg Derzhko and Johannes Richter, “Finite low-temperature entropy of some strongly frustrated quantum spin lattices in the vicinity of the saturation field,” *Physical Review B* **70**, 104415 (2004).
- ⁷⁰ M. E. Zhitomirsky and Hirokazu Tsunetsugu, “Exact low-temperature behavior of a kagomé antiferromagnet at high fields,” *Phys. Rev. B* **70**, 100403 (2004).
- ⁷¹ O. Derzhko, J. Richter, A. Honecker, and H.-J. Schmidt, “Universal properties of highly frustrated quantum magnets in strong magnetic fields,” *Low Temp. Phys.* **33**, 745–756 (2007), <https://doi.org/10.1063/1.2780166>.
- ⁷² J. Jaklič and P. Prelovšek, “Lanczos method for the calculation of finite-temperature quantities in correlated systems,” *Phys. Rev. B* **49**, 5065–5068 (1994).
- ⁷³ J. Jaklič and P. Prelovšek, “Finite-temperature properties of doped antiferromagnets,” *Adv. Phys.* **49**, 1–92 (2000).
- ⁷⁴ Jürgen Schnack and Oliver Wendland, “Properties of highly frustrated magnetic molecules studied by the finite-temperature Lanczos method,” *Eur. Phys. J. B* **78**, 535–541 (2010).
- ⁷⁵ Oliver Hanebaum and Jürgen Schnack, “Advanced finite-temperature Lanczos method for anisotropic spin systems,” *Eur. Phys. J. B* **87**, 194 (2014).
- ⁷⁶ Burkhard Schmidt and Peter Thalmeier, “Frustrated two dimensional quantum magnets,” *Phys. Rep.* **703**, 1 – 59 (2017), frustrated two dimensional quantum magnets.
- ⁷⁷ Roman Schnalle and Jürgen Schnack, “Calculating the energy spectra of magnetic molecules: application of real- and spin-space symmetries,” *Int. Rev. Phys. Chem.* **29**, 403–452 (2010).
- ⁷⁸ Eva Pavarini, Erik Koch, Richard Scalettar, and Richard M. Martin, eds., “The physics of correlated insulators, metals, and superconductors,” (Verlag des Forschungszentrum Jülich, 2017) Chap. The Finite Temperature Lanczos Method and its Applications by P. Prelovšek, ISBN 978-3-95806-224-5.
- ⁷⁹ Jörg Schulenburg, *spinpack 2.56*, Magdeburg University (2017).
- ⁸⁰ As is common praxis, temperatures and energies are given as multiples of J , thereby omitting k_B . $T = 0.67$ thus means $k_B T = 0.67J$.
- ⁸¹ Roderich Moessner and Art Ramirez, “Geometrical frustration,” *Physics Today* **59**, 24–29 (2006).
- ⁸² H.-J. Schmidt, A. Lohmann, and J. Richter, “Eighth-order high-temperature expansion for general Heisenberg hamiltonians,” *Phys. Rev. B* **84**, 104443 (2011).
- ⁸³ Jürgen Schnack, Heinz-Jürgen Schmidt, Johannes Richter, and Jörg Schulenburg, “Independent magnon states on magnetic polytopes,” *Eur. Phys. J. B* **24**, 475 (2001).
- ⁸⁴ Yutaka Shirata, Hidekazu Tanaka, Akira Matsuo, and Koichi Kindo, “Experimental realization of a spin-1/2 triangular-lattice Heisenberg antiferromagnet,” *Phys. Rev. Lett.* **108**, 057205 (2012).
- ⁸⁵ Oleg Derzhko, Johannes Richter, and Mykola Maksymenko, “Strongly correlated flat-band systems: The route from Heisenberg spins to hubbard electrons,” *Int. J. Mod. Phys. B* **29**, 1530007 (2015), <https://doi.org/10.1142/S0217979215300078>.
- ⁸⁶ Johannes Richter, Oleg Derzhko, and Taras Krokhmalkii, “Finite-temperature order-disorder phase transition in a frustrated bilayer quantum Heisenberg antiferromagnet in strong magnetic fields,” *Phys. Rev. B* **74**, 144430 (2006).
- ⁸⁷ Tôru Sakai and Hiroki Nakano, “Novel field-induced quantum phase transition of the kagome-lattice antiferromagnet,” *J. Kor. Phys. Soc.* **63**, 601–604 (2013).
- ⁸⁸ Tian-Heng Han, M. R. Norman, J.-J. Wen, Jose A. Rodriguez-Rivera, Joel S. Helton, Collin Broholm, and Young S. Lee, “Correlated impurities and intrinsic spin-liquid physics in the kagome material herbertsmithite,” *Phys. Rev. B* **94**, 060409 (2016).
- ⁸⁹ Robert Schaffer, Yejin Huh, Kyusung Hwang, and Yong Baek Kim, “Quantum spin liquid in a breathing kagome lattice,” *Phys. Rev. B* **95**, 054410 (2017).
- ⁹⁰ Cécile Repellin, Yin-Chen He, and Frank Pollmann, “Stability of the spin- $\frac{1}{2}$ kagome ground state with breathing anisotropy,” *Phys. Rev. B* **96**, 205124 (2017).
- ⁹¹ Yasir Iqbal, Didier Poilblanc, Ronny Thomale, and Federico Becca, “Persistence of the gapless spin liquid in the breathing kagome Heisenberg antiferromagnet,” *Phys. Rev. B* **97**, 115127 (2018).